Influence of La_2O_3 nanoparticles on Structural, Physical, and Optical Properties of Zinc Lithium Borotellurite glass system

Kiran Nagaraju[1], *Susheela* K Lenkennavar[1*]

[1]Department of Physics, Bangalore University, Bengaluru, Karnataka-560056, India.

Abstract. A series of lanthanum nanoparticles doped with Zinc lithium borotellurite glasses (ZBTLL) was prepared by the melt quenching technique. Physical parameters have been measured and calculated. The effects of lanthanum nanoparticles (La_2O_3) on the structure and optical properties of the glass were studied using various experimental techniques. X-Ray Diffraction (XRD) confirmed that all glass samples were amorphous in nature. Fourier transform infrared (FTIR) spectroscopy studies revealed the presence of borate and tellurite structural units in the glass network which exhibited noticeable variations upon incorporation of La_2O_3 nanoparticles. Optical properties were analysed using UV-Vis spectroscopy. These results indicate that the incorporation of lanthanum nanoparticles modifies the glass network and improving its optical properties and making the materials suitable for optical applications.

1. Introduction:

In the modern world, glass is extensively utilized across various applications. Its special property is the lack of an organized atomic structure, which separates it from crystalline solids and classifies it as an amorphous material [1]. The embedding of rare-earth elements in glass matrices has attracted considerable attention because of their promising applications in optical fibers, waveguide lasers, bulk laser systems, optical amplifiers, and infrared-based photonic devices [2].[1] Borate oxide (B_2O_3) serves as a highly effective medium for rare-earth metal oxides, capable of forming glasses over an extensive compositional range without the need for network-modifying agents. It is considered the leading option for stabilizing glass formation due to its exceptional solubility of rare earth ions and its strength. Borate glasses have a structural framework made up of BO_3 and BO_4 units that interconnect to establish stable borate configurations, including di-borate, tri-borate, and tetra-borate groups [3].
Tellurium oxide (TeO_2) is well known for being an exceptional host matrix, attributed to its remarkable optical characteristics as a good conditional glass former. The presence of modifiers, including alkali, alkaline earth, transition metal oxides, or other glass formers, is essential for TeO_2 to achieve a stable glass state and it enhances infrared transmission and improves glass quality, while also reducing brittleness and bubble formation [4]. By adding zinc oxide (ZnO) to the borotellurite glass composition, the formation of glass is enhanced

*Corresponding author: susheelakl@bub.ernet.in

while the tendency for crystallization is reduced [5]. Incorporating an alkali oxide such as Li_2O leads to the conversion of BO_3 trigonal units into BO_4 tetrahedral units, thus improving the compactness of the glass structure [6]. The presence of La_2O_3 significantly alters the glass matrix by raising its density, thermal expansion, and glass transition temperature, while also lowering the crystallization peak temperature and overall thermal stability [7].
Adding lanthanum oxide into zinc borotellurite glass appears to raise the energy band gap and reduce the Urbach energy within the glass system [8]. The adaptability of borate-based glasses, particularly in relation to the synergistic effects of ZnO and La_2O_3, has enabled the development of materials tailored for demanding technological applications [9]. Thus, through this study, the effect of Lanthanum oxide nanoparticles on the structural, physical, and optical properties of zinc lithium borotellurite glass network will be determined and discussed.

2. Materials and Methodology:

Glasses of composition $25ZnO\text{-}(58\text{-}x)\ B_2O_3\text{-}2TeO_2\text{-}15Li_2O\text{-}xLa_2O_3$. Where (x=0,0.1,0.2,0.3,0.4 mol%) was fabricated by using the Conventional melt quenching technique. The high-purity analytical grade chemicals used are Boric acid (H_3BO_3), Tellurium dioxide (TeO_2), Zinc Oxide (ZnO), Lithium Oxide (Li_2O) and Lanthanum Oxide (La_2O_3) Nanoparticles. The glass codes are given as ZBTLL-0, ZBTLL-0.1, ZBTLL-0.2, ZBTLL-0.3, and ZBTLL-0.4. 10g of the mentioned chemicals were taken and processed into a fine powder using an agate mortar. The even mixture was transferred into a porcelain crucible. The chemical mixture was placed in a porcelain crucible and then introduced to an electric furnace heated to 900^0C for a duration of 2 hours. The transparent melt was poured and rapidly quenched between stainless steel rings to achieve a uniform shape. Following this, the glass samples underwent annealing at 300^0C for 2 hours to reduce thermal strains and enhance their mechanical strength. The glass samples were allowed to reach room temperature and then polished on both sides to achieve a uniform thickness for optical measurements. Furthermore, we were processed into powder for subsequent characterization.

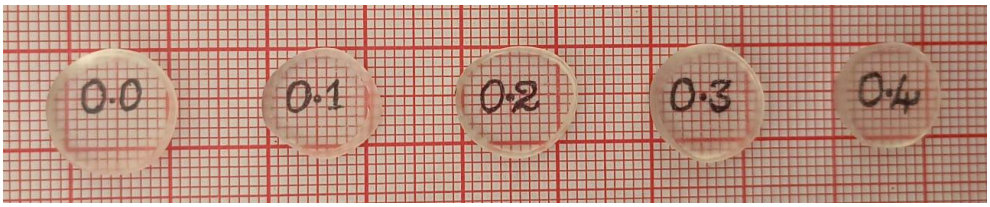

Fig.1 Synthesized ZBTLL glass samples

3. Result and Discussion:

3.1. X-Ray Diffraction (XRD) Spectroscopy:

XRD represents a non-destructive testing method used to determine the presence of crystalline phases in a material through the diffraction and scattering of X-rays as they penetrate the material [10]. Illustrated in **Fig.2** is the XRD pattern obtained from the glass samples in powder form, measured at 2θ angles ranging from 10^0 to 90^0 under room temperature conditions. The absence of sharp peaks confirms the lack of crystalline phases in the samples. The presence of a broad diffuse hump in the XRD pattern indicates that the prepared material is glassy in nature and exhibits typical amorphous characteristics.

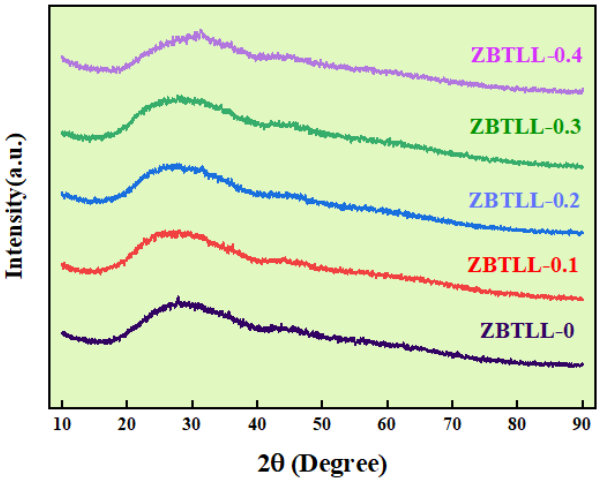

Fig. 2. X-ray diffraction patterns of synthesized ZBTLL glass samples

3.2. Fourier Transform Infra-Red (FTIR) Spectroscopy

Using FTIR spectroscopy, one can reveal the important details about the configuration of the structural components in a glass material [11]. In a glass system, molecules that establish bonds or groups will absorb designated frequencies, resulting in rotation and vibration when the glass samples are analysed through infrared spectroscopy. The FTIR spectra for the synthesized glass sample are shown in **Fig.3**. The broad band positions and assignments are listed in **Table 1.**

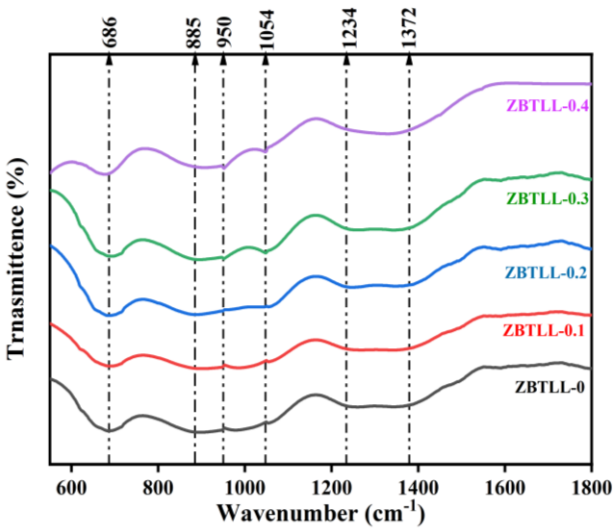

Fig. 3. FTIR spectra of synthesized ZBTLL glass samples

To investigate the structural changes resulting from the addition of La_2O_3 nanoparticles to our glass matrix, we concentrated on the mid-IR region (500-1800 cm^{-1}). The band observed around ~686 cm^{-1} is attributed to Te-O stretching vibration of TeO_3 units, while the bands near ~885 and ~985 cm^{-1} correspond to B-O stretching vibrations of BO_4 units and the presence of non-bridging oxygens (NBOs). The bands around ~1054 cm^{-1} is associated with

B-O, B-O stretching vibrations in BO_4 tetrahedral boron units, indicating borate network participation. The band near ~1234 cm^{-1} is assigned to asymmetric stretching of B-O bonds in trigonal BO_3 groups, whereas the higher-wavenumber band around ~1372 cm^{-1} is related to borate structural rearrangements and increased network disorder. With increasing La_2O_3 content, slight shifts and variations in these bands suggest modification of the borotellurite network, conversion between BO_3 and BO_4 units, and changes in NBO concentration, indicating that lanthanum ions act as network modifiers and influence the glass structure.

Table 1. Assignment of infrared transmission bands for ZBTLL glasses.

Wavenumber (cm^{-1})	Assignment	References
650-700	The stretching vibration of TeO_3 group	[12]
820-906	Stretching vibrations of the B-O bonds in BO_4 units from diborate groups	[13],[14]
911-1110	B-O stretching vibrations in BO_4 tetrahedral boron	[15]
1200-1800	Stretching vibrations of the B-O bonds of BO_3 from different types of borate groups	[16], [17]

3.3. Physical and Optical properties

3.3.1. Density and molar volume:

Density is a vital tool employed to assess the extent of structural compactness of a material [18]. The alteration in the geometric arrangements of the glass system. The density (ρ) value of the glass samples will be used to calculate molar volume (V_m), molar refraction and optical parameters. The density and Molar volume of the glass samples can be obtained by using the following formulas:

$$\rho = \left(\frac{Wa}{Wa-Wb}\right) \rho_b \quad (1)$$

$$V_m = \frac{MW}{\rho} \quad (2)$$

Where, W_a and W_b are weight of glass in air and toluene respectively, ρ_b is density of the toluene, and MW is molecular weight of the glass.

Table 2. Physical Parameters of ZBTLL glasses

Glass Samples	ZBTLL-0	ZBTLL-0.1	ZBTLL-0.2	ZBTLL-0.3	ZBTLL-0.4
Molecular Weight (g/mol)	68.39	68.67	68.94	69.21	69.49
Density (ρ) g/cm^3	2.799	2.853	2.855	2.866	2.869
Molar volume (V_m) cm^3 /mol,	24.43	24.06	24.14	24.14	24.22
Concentration (N_i) (10^{19} ions/cm^3)	_____	5.00	9.97	0.14	0.19
Polaron radius (r_p) nm	_____	1.093	0.868	0.759	0.690
Inter ionic distance (r_i) nm	_____	2.713	2.156	1.883	1.713
Field strength (F)(10^{18}) nm^{-2}	_____	2.508	3.973	5.206	6.294

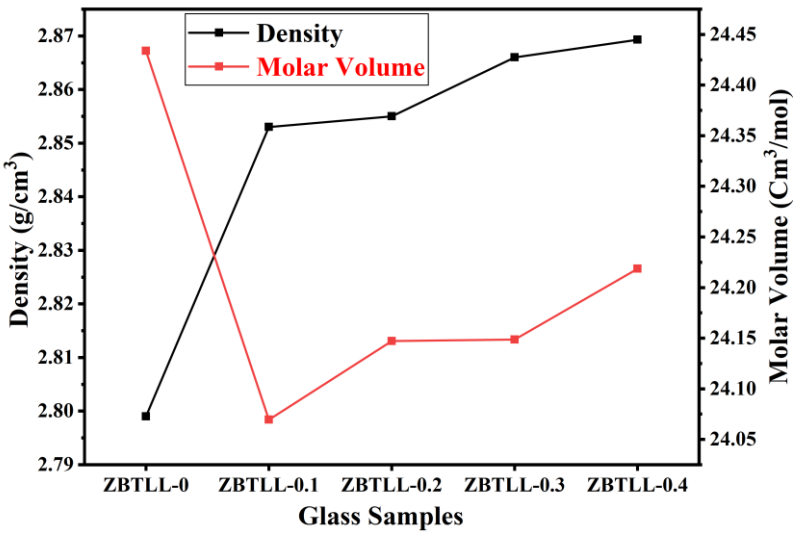

Fig. 4. Density vs Molar Volume of synthesized ZBTLL glass samples

The physical and structural properties of the ZBTLL glass system show a systematic change with increasing La_2O_3 concentration, indicating a gradual modification and compaction of the glass network. The molecular weight and density increase steadily from ZBTLL-0 to ZBTLL-0.4, which is attributed to the incorporation of lanthanum ions and improved packing efficiency within the glass matrix [20] [21]. Adding La_2O_3 leads to decrease in molar volume which indicates less free space and more compact glass structure. The concentration of lanthanum ions increases with doping, therefore the polaron radius and inter-ionic distance decrease, indicating that the ions are packed more tightly and have stronger interactions. The continuous increase in field strength implies that La-O bonds are becoming stronger also improved electrostatic interaction between the modifier ions and the glass structure. These results collectively indicate that La_2O_3 is an effective network modifier, resulting in a borotellurite glass that exhibits increased density and compactness along with improved structural qualities [22].

3.3.2. Optical Absorption

Investigating optical absorption delivers crucial information regarding transitions under optical excitation, as well as the material's band structure and the energy gap associated with it [23]. In crystalline substances, the absorption edge is distinctly sharp, whereas in amorphous substances, the fundamental absorption edge has a gradual slope [24]. **Fig.5** presents the optical absorption spectra for the glass samples in the ultraviolet region having wide range from 300 to 350 nm. Additionally, the shift of the fundamental absorption edge to shorter wavelengths results from the enhanced field strength of the La^{3+} ion with increasing La_2O_3 NP concentration in the glass matrix [25].

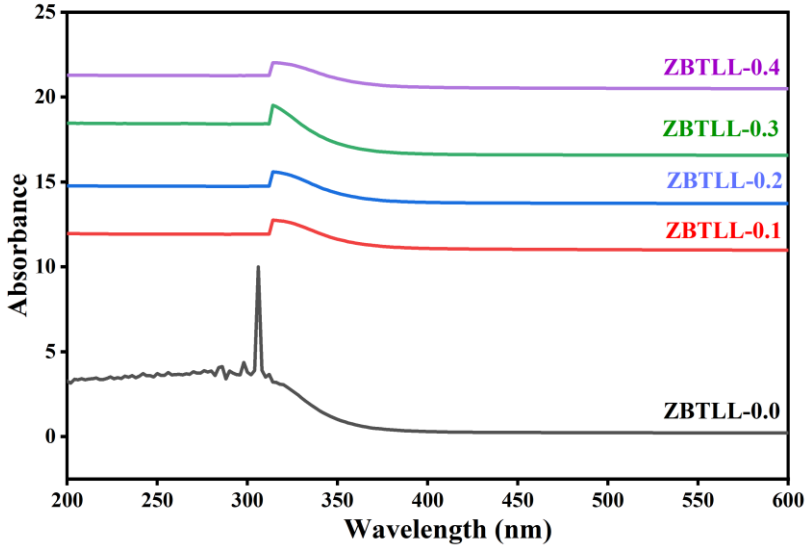

Fig. 5. Optical absorbance spectra of synthesized ZBTLL glass samples

3.3.3. Optical Band Gap

In amorphous materials, optical transitions occurring at the fundamental absorption edge are categorized into two types: one is direct transitions, where the electron's momentum is conserved, and the other is indirect transitions, which require the involvement of a phonon [26]. The calculation can be carried out using models derived from the Tauc method, initially introduced by Davis and Mott, and is represented by the following equation [27].

$$\alpha h\upsilon = B\,(h\upsilon - E_g)^2 \qquad (3)$$

$$(\alpha h\upsilon)^2 = B\,(h\upsilon - Eg) \qquad (4)$$

$$(\alpha h\upsilon)^{1/2} = B\,(h\upsilon - Eg) \qquad (5)$$

Here, we use equations (4) and (5) to calculate direct band gap (E^1_{opt}) and indirect band gap (E^2_{opt}**)** values. where hυ signifies the energy of the photon, B is a constant, E_g refers to the optical band gap, 'n' represents an index that can take on different values (1/2 for indirect transitions and 2 for direct allowed transitions) and α is the absorption coefficient. In **Fig.6**, **7** the E_g Values (direct band gap) for the prepared glass samples are presented **Table 3.** summarises the direct, indirect band gap values, Urbach energy, and refractive index values, indicating a non-linear variation with respect to the concentration of La_2O_3 nanoparticles. The direct optical band gap of the glass samples ranges from 3.44 to 3.56 eV, indicating slight structural changes within a broad band gap amorphous network. Indirect band gap energies ranging from 2.919 to 3.090 eV are lower compared to the direct band gap values of 3.44 to 3.56 eV, which reflects the phonon-assisted transitions typical in disordered glass networks. At intermediate concentrations of 0.3 mole fraction La_2O_3, the energy gap (E_g) increases as a result of enhanced structural compactness. The notable decrease in the energy band gap value can be attributed to a substantial structural alteration that occurred in the glass matrix of the sample containing a 0.4 mole fraction of La_2O_3 nanoparticles.

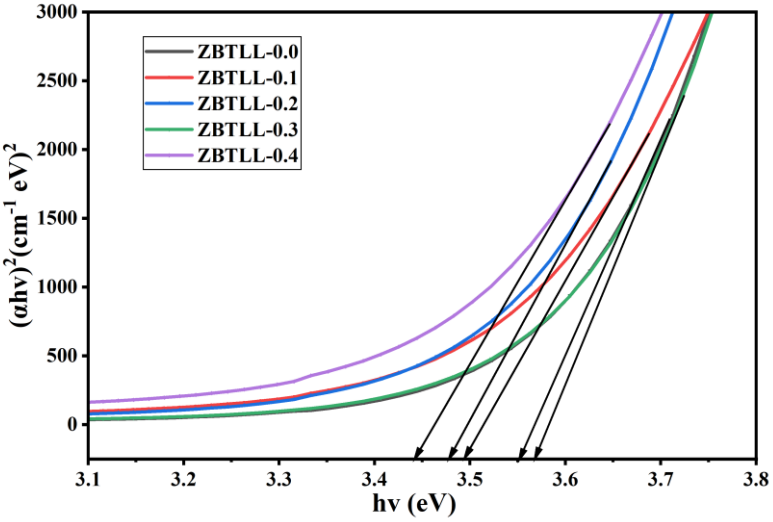

Fig. 6. Direct band gap measurement. Of synthesized ZBTLL glass samples

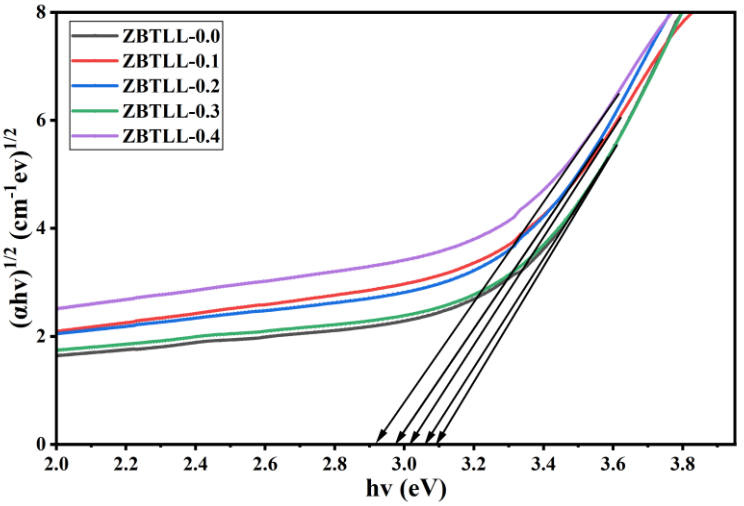

Fig. 7. Indirect band gap measurement of synthesized ZBTLL glass samples

3.3.4. Urbach Energy

In amorphous solids, Urbach energy indicates the level of disorder and the concentration of defects. Materials that possess a higher ΔE value are more likely to change weak bonds into defects [24]. The values of Urbach energy (ΔE) are determined from the slopes of the linear segments in the ln α versus hv plots. An evident reduction in ΔE is seen as the quantity of La_2O_3 NPs in the glass system increases at 0.2 and 0.3 mol%. This downward trend in ΔE correlates with a decrease in the number of defects in the glass matrix. **Fig.8.** represents this.

3.3.5. *Refractive index (n)*

The value of the refractive index in glass is determined by the interaction between light and the electrons of its constituent atoms [28]. The refractive index value of synthesised glass samples are calculated using the formula [29].

$$\frac{n^2-1}{n^2+2} = 1 - \sqrt{\frac{E_g}{20}} \qquad (6)$$

where n is the refractive index and E_g is the value of indirect band gap. Dielectric constant (ε), Reflection loss (R_L), Molar refractivity (R_m), Electronic polarizability (α_e) are calculated using refractive index [19]. **Table 3.**, outlines the particular values of the refractive index (n). The relationship and understanding of the refractive index can be deepened by studying the formation of bridging and non-bridging oxygen in a substance. The results of this study suggest that an increased concentration of La_2O_3 nanoparticles leads to an increase in the refractive index, which can be explained by the presence of high-polarizability Non-bridging oxygen within the glass network. At the same time, the structural changes observed at 0.3 molar fractions of La_2O_3 nanoparticles caused a decreased in the formation of bridging oxygen the trend of both Urbach energy (ΔE) and refractive index vs mole fraction in showed in **Fig.8.**

Table 3. Optical Parameters for ZBTLL glasses.

Glass samples	E^1_{opt} (eV)	E^2_{opt} (eV)	ΔE (eV)	n	ε	R_L (%)	R_m (cm^{-3})	α_e (10^{-24}) (cm^3)
ZBTLL-0	3.55	3.05	0.29	2.262	5.11	8.76	14.13	5.60
ZBTLL-0.1	3.49	3.01	0.34	2.275	5.17	8.89	14.00	5.55
ZBTLL-0.2	3.47	2.97	0.30	2.279	5.19	8.93	14.07	5.58
ZBTLL-0.3	3.56	3.09	0.27	2.258	5.09	8.72	13.94	5.53
ZBTLL-0.4	3.44	2.91	0.37	2.287	5.23	9.01	14.17	5.62

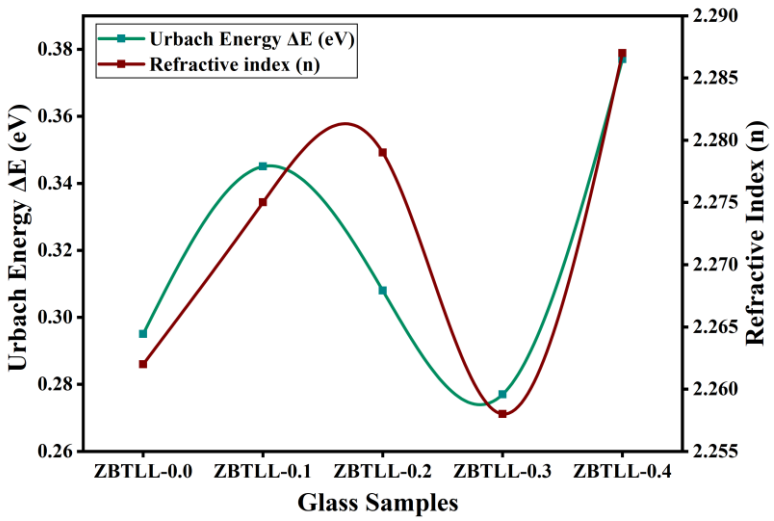

Fig.8. Urbach Energy and Refractive Index of synthesized ZBTLL glass samples

From the above **Table 3.** we come to know the dielectric constant (ε) of La_2O_3 doped ZBTLL glasses increases with lanthanum content due to the incorporation of highly polarizable La^{3+} ions, which enhance the electronic polarization and optical density of the glass network, consistent with the relationship between refractive index and dielectric response [30]. As the refractive index increases, the reflection loss (R_L) also rises, since a higher refractive index leads to stronger Fresnel reflection at the air–glass interface [31]. The observed increase in molar refractivity (R_m) further confirms the enhancement of electronic polarizability and tighter packing of the glass structure with La_2O_3 addition, indicating stronger modifier–oxygen interactions [30].
Correspondingly, the electronic polarizability increases due to the large ionic radius and high polarizing power of La^{3+} ions, which promote stronger La-O bonding and greater deformation of the electron cloud under an applied optical field, a behavior widely reported for lanthanum-containing tellurite and borate glasses. These related trends confirm the effective role of La_2O_3 as a modifier and enhancing optical responses within the borotellurite glass system.

4. Conclusion

Zinc lithium borotellurite glasses doped with lanthanum oxide nanoparticles (ZBTLL) were successfully prepared and systematic investigation was conducted on the structural, physical and optical properties. The XRD patterns confirm the amorphous nature of all prepared samples. FTIR analysis shows that La_2O_3 nanoparticles function as effective network modifiers, enhancing the conversion of BO_3 to BO_4 units and adjusting Te-O bonds which results in a denser and modified borotellurite glass network. The decrease in Urbach energy values indicates that the produced glasses are less brittle in nature. The variations in patterns at 0.2 and 0.4 mol % of La_2O_3 nanoparticles for Urbach energy and refractive index are associated with structural changes in the glass system which improve the formation of non-bridging oxygen. This analysis shows that the doping of La_2O_3 nanoparticles within zinc lithium borotellurite glasses modifies their optical characteristics. The overall results indicate that our prepared ZBTLL glass samples are suitable materials for optical applications.

Acknowledgement

The authors are thankful for the financial support extended by the Vision Group on Science and Technology (VGST), Government of Karnataka, under the scheme KSTEPS/VGST/ECRA/GRD No. 1251/2023-24.

References

1. W. D. Callister, D. G. Rethwisch, Materials science and engineering: SI version. Wiley (2011).
2. H. Lin, D. Yang, G. Liu, T. Ma, B. Zhai, Q. An, J. Yu, X. Wang, X. Liu, E. Y. Pun, Optical absorption and photoluminescence in Sm^{3+}- and Eu^{3+}-doped rare-earth borate glasses. J. Lumin. 113, 121–128 (2004). https://doi.org/10.1016/j.jlumin.2004.09.115
3. K. Maheshvaran, P. Veeran, K. Marimuthu, Structural and optical studies on Eu^{3+} doped boro-tellurite glasses. Solid State Sci. 17, 54–62 (2012). https://doi.org/10.1016/j.solidstatesciences.2012.11.013
4. M. K. Halimah, W. M. Daud, H. A. A. Sidek, A. W. Zaidan, A. S. Zainal, Optical properties of ternary tellurite glasses. Mater. Sci. Pol. 28, 173–180 (2010).

5. M. R. Dousti, S. R. Hosseinian, Enhanced upconversion emission of Dy^{3+} -doped tellurite glass by heat-treated silver nanoparticles. J. Lumin. 154, 218–223 (2014). https://doi.org/10.1016/j.jlumin.2014.04.028
6. N. S. Prabhu, V. Hegde, A. Wagh, M. Sayyed, O. Agar, S. D. Kamath, Physical, structural and optical properties of Sm^{3+} doped lithium zinc alumino borate glasses. J. Non-Cryst. Solids 515, 116–124 (2019). https://doi.org/10.1016/j.jnoncrysol.2019.04.015
7. Y. S. Hordieiev, A. V. Zaichuk, Lanthanum-doped zinc borate glasses: fabrication, structural analysis, thermal properties, and gamma radiation shielding performance. J. Ovonic Res. 21, 85–94 (2025). https://doi.org/10.15251/jor.2025.211.85
8. F. M. Fudzi, H. M. Kamari, F. D. Muhammad, A. A. Latif, Z. Ismail, Structural and optical properties of zinc borotellurite glass co-doped with lanthanum and silver oxide. J. Mater. Sci. Chem. Eng. 6, 18–23 (2018). https://doi.org/10.4236/msce.2018.64003
9. H. Lin, X. Zhao, W. Chen, L. Luo, Formation and thermal properties of B_2O_3–La_2O_3–ZnO glasses for low temperature co-fired ceramics. J. Alloys Compd. 479, 859–862 (2009). https://doi.org/10.1016/j.jallcom.2009.01.082
10. A. Usman, M. K. Halimah, A. Latif, F. D. Muhammad, A. Abubakar, Influence of Ho^{3+} ions on structural and optical properties of zinc borotellurite glass system. J. Non-Cryst. Solids 483, 18–25 (2018). https://doi.org/10.1016/j.jnoncrysol.2017.12.040
11. M. Farouk, A. Samir, M. E. Okr, Effect of alkaline earth modifier on the optical and structural properties of Cu^{2+} doped phosphate glasses as a bandpass filter. Physica B. 530, 43–48 (2017). https://doi.org/10.1016/j.physb.2017.11.013
12. F. M. Fudzi, H. M. Kamari, M. N. A. Azis, Effect of lanthanum oxide on optical properties of zinc borotellurite glass system. J. Optoelectron. Biomed Mater. 8, 1–6 (2016).
13. A. Azuraida, M. K. Halimah, M. Ishak, L. Hasnimulyati, S. I. Ahmad, Gamma ray shielding parameter of barium-boro-tellurite glass. Chalcogenide Lett. 17, 187–196 (2020). https://doi.org/10.15251/cl.2020.174.187
14. Y. Rammah, A. Ali, R. El-Mallawany, F. El-Agawany, Fabrication, physical, optical characteristics and gamma-ray competence of novel bismo-borate glasses doped with Yb_2O_3 rare earth. Physica B 583, 412055 (2020). https://doi.org/10.1016/j.physb.2020.412055
15. C. M. Reddy, B. D. P. Raju, N. J. Sushma, N. Dhoble, S. Dhoble, A review on optical and photoluminescence studies of RE^{3+} ions doped LCZSFB glasses. Renew. Sustain. Energy Rev. 51, 566–584 (2015). https://doi.org/10.1016/j.rser.2015.06.025
16. N. Elkhoshkhany, H. M. Mohamed, E. S. Yousef, UV–Vis–NIR spectroscopy, structural and thermal properties of novel oxyhalide tellurite glasses for optical application. Results Phys. 13, 102222 (2019). https://doi.org/10.1016/j.rinp.2019.102222
17. M. Halimah, L. Hasnimulyati, A. Zakaria, S. Halim, M. Ishak, A. Azuraida, N. M. Al-Hada, Influence of gamma radiation on the structural and optical properties of thulium-doped glass. Mater. Sci. Eng. B. 226, 158–163 (2017). https://doi.org/10.1016/j.mseb.2017.09.010
18. Y. Saddeek, K. Aly, K. Shaaban, A. M. Ali, M. M. Alqhtani, A. M. Alshehri, M. Sayed, E. A. Wahab, Physical properties of B_2O_3–TeO_2–Bi_2O_3 glass system. J. Non-Cryst. Solids 498, 82–88 (2018). https://doi.org/10.1016/j.jnoncrysol.2018.06.002
19. M. K. Halimah, W. H. Chiew, H. A. A. Sidek, W. M. Daud, Z. A. Wahab, A. M. Khamirul, S. M. Iskandar, Physical and optical properties of tellurite-based glasses. Sains Malaysiana 43, 889–896 (2014).

20. S. K. Lenkennavar, Effect of rare earth impurities on physical, structural and optical properties of borate-based glasses. J. Sci. Res. 65, 8–15 (2021).
21. A. Paul, *Chemistry of Glasses*, 2nd ed. Chapman & Hall, London (1990).
22. J. E. Shelby, *Introduction to Glass Science and Technology*, 2nd ed. Royal Society of Chemistry, Cambridge (2005).
23. V. Dimitrov, T. Komatsu, Electronic polarizability, optical basicity and non-linear optical properties of oxide glasses. J. Non-Cryst. Solids 249, 160–179 (1999). https://doi.org/10.1016/S0022-3093(99)00317-8
24. A. A. Higazy, A. Hussein, Optical absorption studies of γ-irradiated magnesium phosphate glasses. Radiat. Eff. Defects Solids. 133, 225–235 (1995). https://doi.org/10.1080/10420159508223993
25. S. El-Rabaie, T. Taha, A. Higazy, Non-linear optical and electrical properties of germanate glasses. Physica B 429, 1–5 (2013). https://doi.org/10.1016/j.physb.2013.07.029
26. K. Terashima, S. Tamura, S. Kim, T. Yoko, Structure and nonlinear optical properties of lanthanide borate glasses. J. Am. Ceram. Soc. 80, 2903–2909 (1997). https://doi.org/10.1111/j.1151-2916.1997.tb03210.x
27. C. A. Hogarth, E. Assadzadeh-Kashani, Optical properties of tungsten–calcium–tellurite glasses. J. Mater. Sci. 18, 1255–1263 (1983). https://doi.org/10.1007/BF00551995
28. E. A. Davis, N. F. Mott, Conduction in non-crystalline systems V. Conductivity, optical absorption and photoconductivity in amorphous semiconductors. Philos. Mag. 22, 903–922 (1970). https://doi.org/10.1080/14786437008221061
29. R. El-Mallawany, M. D. Abdalla & I. A. Ahmed, New tellurite glass: Optical properties. Mater. Chem. Phys. **109**, 291–296 (2008). https://doi.org/10.1016/j.matchemphys.2007.11.040
30. V. Dimitrov & T. Komatsu, Electronic polarizability, optical basicity and non-linear optical properties of oxide glasses. J. Non-Cryst. Solids **249**, 160–179 (1999). https://doi.org/10.1016/S0022-3093(99)00317-8
31. M. Born & E. Wolf, *Principles of Optics*, 7th ed., Cambridge Univ. Press (1999).